



# Integration of biocompatible hydrogen evolution catalyst developed from metal-mix solutions with microbial electrosynthesis

Sanne M. de Smit<sup>a,b</sup>, Thomas D. van Mameren<sup>a</sup>, Koen van Zwet<sup>a</sup>, H. Pieter J. van Veelen<sup>c</sup>, M. Cristina Gagliano<sup>c</sup>, David P.B.T.B. Strik<sup>a,\*</sup>, Johannes H. Bitter<sup>b,\*</sup>

<sup>a</sup> Environmental Technology, Wageningen University and Research, Wageningen, The Netherlands

<sup>b</sup> Biobased Chemistry and Technology, Wageningen University and Research, Wageningen, The Netherlands

<sup>c</sup> Wetsus, European Centre of Excellence for Sustainable Water Technology, Leeuwarden, The Netherlands

## ARTICLE INFO

### Keywords:

Microbial electrosynthesis  
CO<sub>2</sub> reduction  
Hydrogen evolution catalyst  
Microbial trace nutrients  
Microbial chain elongation

## ABSTRACT

Microbial conversion of CO<sub>2</sub> to multi-carbon compounds such as acetate and butyrate is a promising valorisation technique. For those reactions, the electrochemical supply of hydrogen to the biocatalyst is a viable approach. Earlier we have shown that trace metals from microbial growth media spontaneously form in situ electrocatalysts for hydrogen evolution. Here, we show biocompatibility with the successful integration of such metal mix-based HER catalyst for immediate start-up of microbial acetogenesis (CO<sub>2</sub> to acetate). Also, *n*-butyrate formation started fast (after twenty days). Hydrogen was always produced in excess, although productivity decreased over the 36 to 50 days, possibly due to metal leaching from the cathode. The HER catalyst boosted microbial productivity in a two-step microbial community bioprocess: acetogenesis by a BRH-c20a strain and acetate elongation to *n*-butyrate by *Clostridium sensu stricto* 12 (related) species. These findings provide new routes to integrate electro-catalysts and micro-organisms showing respectively bio and electrochemical compatibility.

## 1. Introduction

Catalysis is key to the sustainable production of chemicals, materials & fuel in the future. For the conversion of CO<sub>2</sub> into valuable chemicals, use of microbial catalysts widens the product spectrum while improving selectivity[1]. During this bio-electrochemistry process, the mixed microbial community catalyses CO<sub>2</sub> reduction in an electrosynthesis cell leading to the formation of green chemical products (like ethanol[2], methane[3], ethylene[4]) and medium chain fatty acids (acetate, butyrate, caproate)[5–9]. Medium chain fatty acids (MCFAs) have many applications, ranging from antimicrobials to precursor for bioplastics or biofuels[10].

These conversions are anaerobic processes driven by electroactive bacteria, which grow in suspension and/or form a biofilm on the cathode. Electrons are generated at the anode, charged by an external energy source and supplied to the microbial community on the cathode, directly or via a carrier such as hydrogen[11,12]. These bio-electrochemical CO<sub>2</sub> reductions can be performed with non-aseptic microbial cultures which is promising for the treatment of different kind of CO<sub>2</sub>-rich waste

streams[13]. MCFAs production with open cultures of microbial consortia is possible via chain elongation, where during anaerobic fermentation the short-chain carboxylates can be elongated via different pathways[14]. A first step of the elongation process is the formation of acetate from two molecules of CO<sub>2</sub> during homoacetogenesis[15]. For bio-electrochemical acetogenesis, hydrogen was shown to be an intermediate in the electron transport between the cathode and the bacteria[11]. Previous studies showed that bio-electrochemical acetogenesis productivity was stimulated by improved hydrogen supply[16,17]. Therefore, it is hypothesized that stimulating hydrogen production from the start of the bio-electrochemical chain elongation process would benefit the production of medium chain fatty acids. To date, the highest hydrogen supply rates in microbial electrosynthesis required long start-up times (>100 days) leading to current densities at maximum –13kA/m<sup>3</sup> [6].

Hydrogen formation at the electrode surface (hydrogen evolution reaction) can be stimulated by the incorporation of a chemical catalyst. To combine a chemical hydrogen evolution reaction (HER) catalyst with a microbial catalyst in the same system, it is essential that the HER

\* Corresponding authors.

E-mail addresses: [david.strik@wur.nl](mailto:david.strik@wur.nl) (D.P.B.T.B. Strik), [harry.bitter@wur.nl](mailto:harry.bitter@wur.nl) (J.H. Bitter).

<https://doi.org/10.1016/j.bioelechem.2024.108724>

Received 29 November 2023; Received in revised form 29 April 2024; Accepted 1 May 2024

Available online 3 May 2024

1567-5394/© 2024 The Authors. Published by Elsevier B.V. This is an open access article under the CC BY license (<http://creativecommons.org/licenses/by/4.0/>).

catalyst functions under conditions suitable for microbial electrosynthesis, e.g. near neutral pH and in mild temperature ranges[18,19]. Several studies have reported HER catalysts which catalyse hydrogen formation under microbial compatible conditions. These studies used for example Pt, Co, Mo or Ni-based catalysts that required specific methods to integrate them on the cathode[20–25]. Recently, de Smit et al. [26] showed the highest reported hydrogen production rates (up to 11 kg H<sub>2</sub> d<sup>-1</sup> m<sup>-3</sup> cathode) with a HER catalyst generated from feeding a trace metal mix solution and EDTA (TMM+) in an electrochemical system without microorganisms, but with microbial compatible conditions (bulk pH 5.8, 30 °C). In that work, the generation of such catalyst was possible thanks to a pre-treatment by the addition of a 100x concentrated trace metal solution (Co, Cu, Mn, Mo, Ni and Zn in solution with ethylenediaminetetraacetic acid EDTA) into the salt electrolyte (phosphate buffer, Mg and Ca salts) in the cathode compartment of the reactor [26].

Although the preliminary findings were promising, it remains unknown whether microbial electrosynthesis is compatible with a TMM based catalyst. Because it would require addition of high concentrations of trace metals to the electrochemical reactors, the conditions can be toxic for microorganisms and inhibit their growth[27]. Regarding toxicity, not only the influence of the metal elements, but also the effect of EDTA should be considered, because EDTA can lower metal toxicity [28]. Another factor to consider for the combination of a HER catalyst and microbial activity is that hydrogen bubble formation can cause shear stress at the cathode surface and thus inhibit biofilm formation [16]. Besides the effects of the HER catalyst on the biofilm, the biofilm can also affect the HER catalyst performance. For example, the growth of microorganisms can cause uptake of the deposited trace metals from the cathode[29–33], which reduces the amount of available HER catalyst.

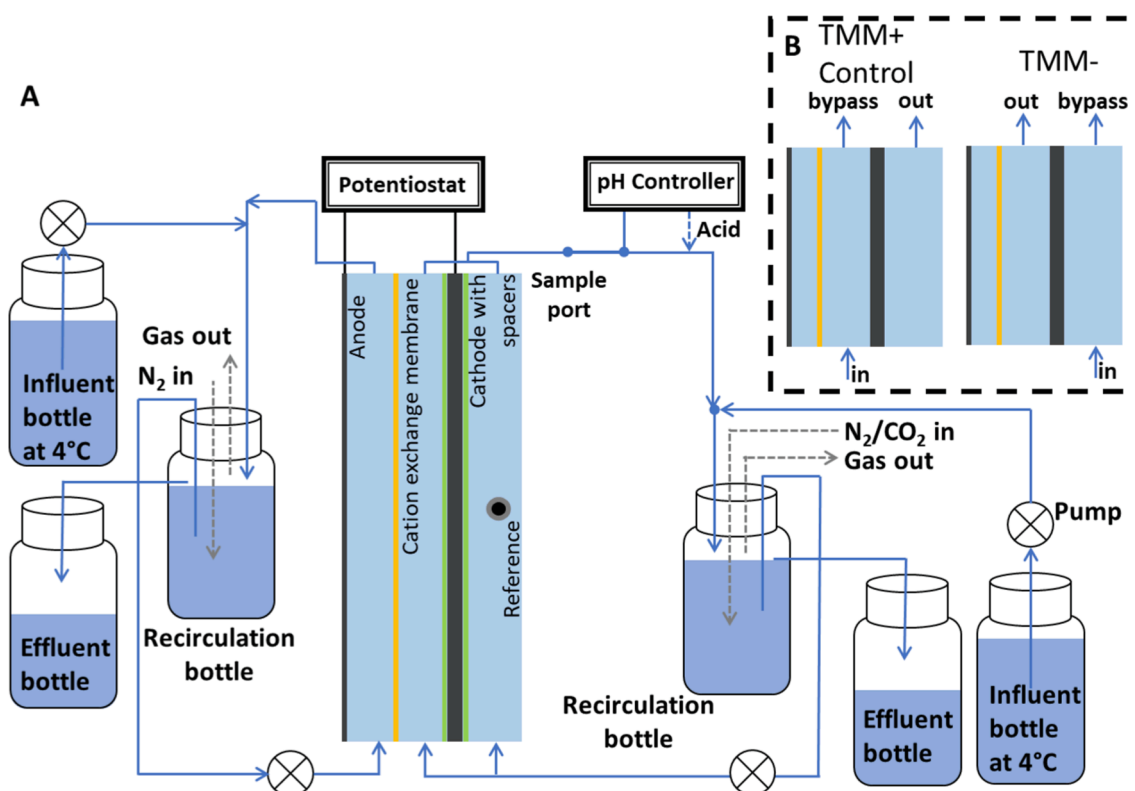
The aim of this study was to evaluate the feasibility of combining a trace metal mix HER catalyst with microbial electrosynthesis. The HER catalyst was deposited on the cathode using the trace metal mix with (TMM+) and without (TMM-) EDTA. The system was evaluated for bio-

electrochemical CO<sub>2</sub> elongation systems. To this purpose, mixed microbial cultures were added to bio-electrochemical systems after pre-treatment with the trace metal mix. First, the formed catalyst was evaluated based on productivity and stability. Second, the activity and composition of the microbial community was investigated. This study presents a successful first integration of an in situ HER catalyst generated from trace metals solution reached a record of -90 kA/m<sup>3</sup> and a CO<sub>2</sub>-utilizing microbial community in the same bio-electrochemical chain elongation system.

## 2. Experimental

### 2.1. Reactor setup & operation

Two sets of duplicate reactors were used for this study. The reactor setup was assembled with Plexiglass flow-through plates (14 mm), with one for the anodic chamber (30 mL) and two for the cathodic chamber (60 mL) (Scheme 1) and placed in a temperature controlled (30 °C) and light-shielded cabinet. The reactors consisted of a Ti/Pt-Ir MMO anode (thickness 1 mm, Magneto Special Anodes BV, Netherlands) and one layer (3 mm) graphite felt cathode (Rayon Graphite Felt, CTG Carbon GmbH, Germany), secured with spacers in the Plexiglas flow-through plates with 21.3 cm<sup>2</sup> projected surface area. The graphite felt was non-microporous with a surface area < 1 m<sup>2</sup>/g, as determined by N<sub>2</sub> physisorption. The cathode current collector consisted of a titanium wire (0.8 mm, grade 2). The cathode potential was controlled at -1.06 V vs an Ag/AgCl reference electrode (3 M KCl, QM710X, Q-is, the Netherlands) over the whole course of the experiment by a n-stat potentiostat (IVIUM, the Netherlands). The anode and cathode compartment were separated by a cation exchange membrane (Fumasep FKS, Fumatech BWT GmbH, Germany, 21.3 cm<sup>2</sup> projected surface area). The total recirculation volumes of the anolyte and catholyte were respectively 339–365 and 391–408 mL. Both anolyte and catholyte were continuously recirculated at respectively 10 and 17 L/h. CO<sub>2</sub> was added



**Scheme 1.** Overview of reactor setup, adapted from de Smit et al., 2022 (A) and recirculation flow-through configuration for different experimental sets (B). Liquid flows are indicated with blue arrows and gas flows are indicated with grey dashed arrows. The graphite felt cathode was secured in place with spacers (green)

in gaseous form in a 30:70 CO<sub>2</sub>:N<sub>2</sub> mix, with 100 LN/d CO<sub>2</sub>, which was sparged (sparger head 22 mm height, 12 mm diameter) into the catholyte recirculation bottle (Scheme 1). The CO<sub>2</sub>:N<sub>2</sub> gas mix was flushed through a demi water bottle prior to entering the reactors to ensure the gas stream was humidified. The anolyte recirculation bottle was continuously sparged with 60 LN/d N<sub>2</sub> to remove excess O<sub>2</sub>. Previous studies showed hydrogen gas build-up between the cathode and the membrane, so a bypass was installed to release gas (Scheme 1B). Flow measurements revealed that 46–88 % of the total catholyte recirculation flow passed through the bypass. In the catholyte recirculation loop, a pH controller (Ontwikkelwerkplaats, Elektronica ATV, the Netherlands) with measuring probe (QMP108X, Q-is, the Netherlands) was installed to maintain the pH of the recirculated catholyte at 5.8.

## 2.2. Reactor pretreatment

To test the effect of the presence of a trace metal mix-based catalyst on microbial growth and activity, two sets of reactors were pre-treated with a trace metal mix. In Table 1, the three separate phases of the experiment are shown, with the corresponding medium compositions in SI Table S1 and S2. After 1–7 days of operation with “blank medium” without trace metals or ammonium (SI Table S1), 10 vol% concentrated trace metal mix solution (SI Table S2) was added to the reactor catholyte with a syringe, to start the “Metal phase”. One set of cathodes was pre-treated with a trace metal mix without EDTA (TMM–), since the omission of EDTA was expected to result in better deposition of trace metal elements to the cathode and thus better catalyst formation. The TMM– mix was added as a suspension which was continuously stirred during the aspiration with the syringe. Another set of reactors was pre-treated with the trace metal mix with EDTA (TMM+). The trace metal mix compositions are shown in SI Table S2. The reactor was left in batch mode during several days to allow the metals to deposit on the cathode. The incubation time with concentrated metals for the experiments with TMM+ and TMM– were respectively 10 and 2 days (Table 1).

The incubation time for the TMM– was shorter because the metals disappeared from the solution more rapidly (SI Figure S2). After incu-

$$\text{Hydrogen conc} [\mu\text{M}] = 7.7 \cdot 10^{-6} \frac{\text{mol}}{\text{m}^3 \text{Pa}} * 101325 \text{ Pa} * \frac{\text{fraction}_{\text{offgas}} \text{H}_2 [\%]}{100\%} * 10^3 \frac{\mu\text{mol} * \text{m}^3}{\text{L} * \text{mol}} \quad (1)$$

bation time, the “biotic phase” was started in the reactors, by flushing the electrolytes with three times the total catholyte volume of anaerobic biotic medium composed of NH<sub>4</sub> and biocompatible low concentration of trace metals (in a mix with EDTA) (SI Table S1). In contrast with previous research[6,34], the biotic medium used in this study did not contain methanogenesis inhibitor 2-bromoethanesulfanoate. Reason for this was suspicion that this sulphur-containing compound could poison the catalyst as seen in literature[35] and preliminary study which showed current decrease simultaneous with sulphur deposition on the cathode in the presence of 2-bromoethanesulfanoate (SI Figure S1). Right after this replacement of the electrolytes, the reactors were inoculated with 10 vol% catholyte with a mixed microbial culture which was

**Table 1**

Duration and medium used in each phase of the biotic experiments. The medium compositions are shown in SI Table S1 and S2.

Phase	HRT catholyte (d)	Metal mix with EDTA (TMM+)		Metal mix without EDTA (TMM–)		Control	
		Medium	Duration (d)	Medium	Duration (d)	Medium	Duration (d)
Blank phase	Batch	Blank medium	7	Blank medium	1	–	–
Metal phase	Batch	TMM+	10	TMM–	2	–	–
Biotic phase	14	Biotic medium	36	Biotic medium*	48	Biotic medium	29

\* Catholyte inflow port changed (Scheme 1B).

previously grown with similar conditions (bio-electrochemical CO<sub>2</sub>-fed system, bulk pH 5.8, –200 mA to graphite felt cathode, 30 °C) and showed production of fatty acids (C2-C4). Inoculation was repeated on day 24, 31 and 38 for the TMM+ experiments and on day 25 and 36 for the TMM– experiments. During the biotic phase, the catholyte medium feed was changed from batch to continuous with a hydraulic retention time (HRT) of 14 days. The anolyte medium feed on the other hand, was continuously fed to the reactor with HRT 4 days, to prevent depletion of anolyte (Table 1).

One set-up adjustment was made for the biotic phase of the experiments without EDTA in the pre-treatment mix (TMM–), the cathode inflow port and the position of the bypass were changed to allow for better mixing of the catholyte chamber (Scheme 1B, Table 1). For the other two runs (TMM+ and control), the cathode chamber inflow port was positioned between the membrane and the cathode (Scheme 1B).

## 2.3. Analytical methods

To analyse formation of various products and catalyst stability, several analysis methods were applied. Gas chromatography was applied to analyse the gas phase and for measuring fatty acids and alcohols in the liquid phase, according to the method described in the SI.

To evaluate the microbial growth in the liquid fraction, 1 mL of sample was mixed and analysed at a wavelength of 600 nm via a Hach spectrophotometer (DR3900, Hach Lange, Germany). Metal concentrations on the cathode, titanium wire and in the catholyte were measured by an inductively coupled plasma analyzer (ICP-OES, Perkin Elmer AVIO 500) as described by de Smit, Buisman, Bitter and Strik [34] with adjustments described in the SI.

## 2.4. Calculations

The hydrogen concentration in the catholyte was calculated based on the measured hydrogen fraction in the off gas (fraction<sub>offgas</sub> H<sub>2</sub>), based on a Henry coefficient of 7.7E-06 mol/(m<sup>3</sup>Pa)[36] and a pressure of 1 atm (101325 Pa) (Equation (1)):

The electron recovery into volatile fatty acids (η<sub>VFA,s</sub>) and hydrogen (η<sub>H<sub>2</sub></sub>) was calculated based on the measured current at the sampling time (Current<sub>t</sub>) in mA (mC/s), the catholyte outflow rate at the sampling time (Q<sub>t</sub>, calculated based on the inflow rate and acid addition over time), and the measured concentrations of volatile fatty acids in the liquid phase at the sampling time Conc<sub>VFA,t</sub> (Equation (2)):

$$\eta_{VFA,s} = \frac{96485 \frac{\text{mC}}{\text{mmol e}^-} * \text{Conc}_{VFA,t} \left[ \frac{\text{mmol}}{\text{L}} \right] * Q_t \left[ \frac{\text{L}}{\text{h}} \right] * X_{\text{mmol e}^-}}{\text{Current}_t \left[ \frac{\text{mC}}{\text{s}} \right] * 3600 \frac{\text{s}}{\text{h}}} \quad (2)$$

The hydrogen flow was calculated based on the hydrogen and

nitrogen fractions in the measured off gas (fraction<sub>offgas</sub>H<sub>2</sub>, fraction<sub>offgas</sub>N<sub>2</sub>), the reactor temperature (Temp) and the ideal gas law, assuming that the N<sub>2</sub> was inert inside the reactors (Equation (3)):

$$Flow_{H_2} \left[ \frac{mmol H_2}{h} \right] = \frac{fraction_{offgas} H_2 [\%] * 233.3 \frac{LN N_2}{d}}{fraction_{offgas} N_2 [\%] * 24 \frac{h}{d}} * \frac{101325 Pa}{8.314 \frac{J}{K * mol} * Temp [K]} \quad (3)$$

The electron recovery into hydrogen was calculated based on the hydrogen flow and the current measured at the sampling time of the hydrogen (Equation (4)):

$$\eta_{H_2} = \frac{96485 \frac{mC}{mmol e^-} * Flow_{H_2} \left[ \frac{mmol H_2}{h} \right] * 2 \frac{mmol e^-}{mmol H_2}}{Current_t \left[ \frac{mC}{s} \right] * 3600 \frac{s}{h}} \quad (4)$$

## 2.5. Microbial community analysis

### 2.5.1. Sample collection and DNA extraction

At the end of the biotic experiments, liquid samples were collected from each reactor and stored at  $-20^\circ C$  to investigate the microbial community composition via DNA extraction and Next Generation Sequencing of 16S rRNA gene. DNA was extracted using the Powersoil DNA isolation kit (Qiagen, USA) according to the manufacturer's instructions. DNA concentration and purity were measured with the NanoDrop spectrophotometer (Thermo Fisher Scientific, Germany).

Sequencing of 16S rRNA genes and bioinformatics.

DNA extracts (18.6–25.3 ng/ml) were sent to MrDNALab (Shallowater, TX, USA) for library preparation and 16S rRNA gene amplicon sequencing as described in the SI. Raw sequence data were processed with QIIME2 (v. 2019.10) [37] as described in SI. For the data presented in this study, we considered the most significant genera per each sample

out of the total number of sequences, setting a cut-off value of 3 %. Microbiota raw sequencing data are submitted to the ENA database (<https://www.ebi.ac.uk/ena>) under accession number PRJEB55693.

### 2.5.2. Fluorescent in situ hybridization (FISH)

For FISH analysis, cathode samples carrying biofilm were fixed with 170  $\mu$ l 37 % formaldehyde. After fixation, samples were stored at  $-20^\circ C$  in 3 ml of ethanol/PBS (1:1). To improve the procedure efficiency, the cathode biofilm was pre-treated via sonication (40 kHz, 50 W, room temperature) in three cycles of 20 s with 10 s pauses during which the samples were kept in ice, in order to disaggregate the cell clusters. The sonicated samples were used for FISH analysis following the protocol of Hugenholtz, Tyson and Blackall [38]. All oligonucleotide probes applied, labelled with Cy3-red or Alexa488-green fluorophores, are listed in SI Table S3. Oligonucleotide probes were selected based on the NGS data and the probeBASE database [39]. Samples were examined using an epifluorescence microscope BX43 (Olympus, Japan) equipped with a DP80 digital camera and the cellSens Standard imaging software (Olympus, Japan). For the image analysis, the FIJI software package (version 1.51 g, Wayne Rasband, NIH, Bethesda, MD, United States) was used.

### 2.5.3. Scanning electron microscopy (SEM)

To analyse the structure of the attached biofilm growing on the cathode, Scanning Electron Microscopy (SEM) was applied. Sample preparation was performed as described in SI. The SEM images were obtained with a Magellan 400 SEM (FEI Company, Hillsboro, OR, USA) at an acceleration voltage 2 kV and beam current of 13 pA at RT.

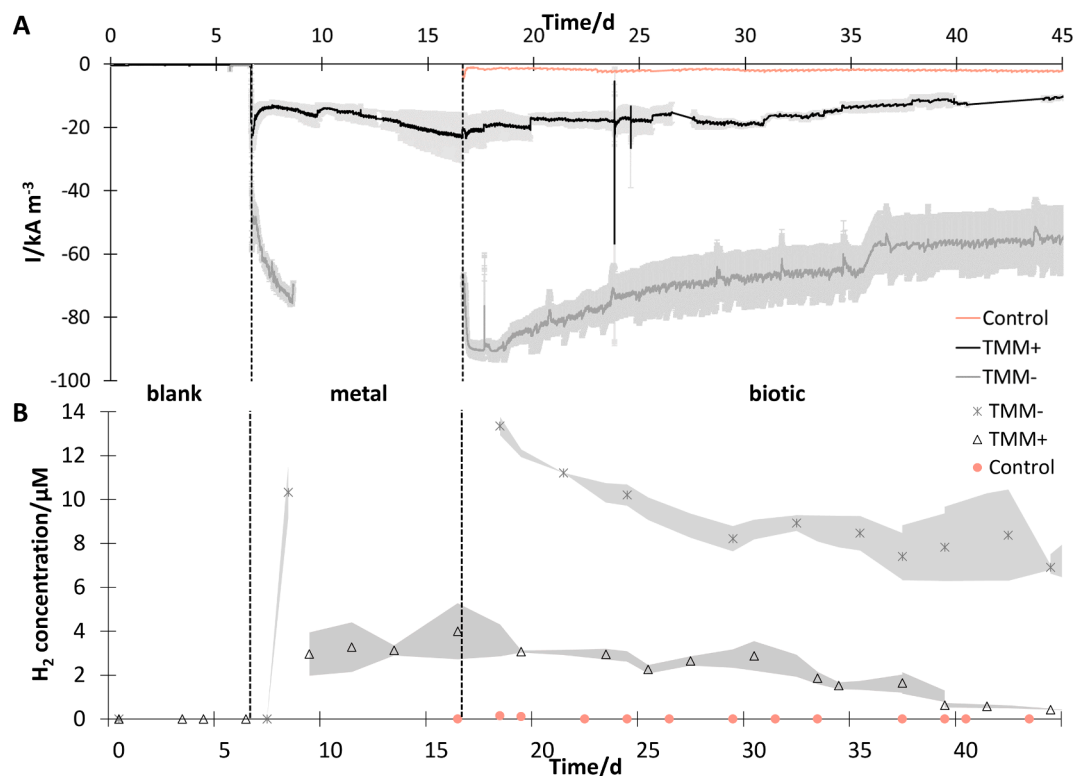


**Fig. 1.** Cathodic current increase (A) and catholyte hydrogen concentration (B) after deposition of trace metal mix solutions with (TMM+, black line) and without (TMM-, grey line) EDTA (day 7–17, metal phase), compared to a blank phase without trace metals (day 0–7, blank) and during the biotic phase with biotic conditions and microorganisms (day 17–45, biotic), compared to a control experiment without pre-treatment (control). The standard deviation between duplicate experiments is shown as grey areas. The reactors were operated at  $-1.06$  V vs Ag/AgCl throughout the whole experiment.

### 3. Results and discussion

#### 3.1. Trace metal mix pre-treatment generates hydrogen evolution catalyst

To investigate the effect of cathode pre-treatment on the electron availability for the microbial consortia, the performances of duplicate cathodes pre-treated with trace metal mix with (TMM+) and without EDTA (TMM-) were evaluated via current and hydrogen measurement. Fig. 1 shows the hydrogen production and observed currents for a blank reactor without added metal mix, after metal addition (day 7) and after inoculation with active biomass (day 17). For the reactors pre-treated with the TMM- mixture, the biotic phase was started 2 days after addition of the metal mixture, since the current was observed to be stable after the initial 2 days for the TMM+ pre-treatment. In Fig. 1, the current and hydrogen production data are normalized by the starting days of the different phases (blank, metal, biotic). For comparison, a control reactor was started after 17 days (Fig. 1 red line). At a constant potential ( $-1.06$  V), the resulting current varied significantly over the different experiments. Right after the addition of the metal mixes (day 7), the current increased to  $-20$  kA/m<sup>3</sup> for the TMM+ experiments, while the TMM- experiments showed a current increase to  $-75$  kA/m<sup>3</sup> (Fig. 1A). In the biotic phase (with presence of micro-organisms), the high current rates were maintained despite the catholyte replacement with biotic medium (day 17). The current even increased to  $-90$  kA/m<sup>3</sup> ( $-27$  mA/cm<sup>2</sup>) for the TMM- experiments at the start of the biotic phase.

The current values were 10 and 40 times higher than measured in the control experiment without pre-treatment (red line, Fig. 1A). The current increases correspond with increases in the hydrogen concentrations (Fig. 1B). The hydrogen concentration in the recirculated catholyte reached 4 and 13.3  $\mu$ M respectively the TMM+ and TMM- experiments (maximum solubility is 718  $\mu$ M[40]), whilst the maximum hydrogen concentration in the control experiment was 0.15  $\mu$ M (Fig. 1B).

The current after the metal mix pre-treatment was substantially higher compared to the control experiment, where the current started at  $-1$  kA/m<sup>3</sup> and increased to  $-2$  kA/m<sup>3</sup> during the 28 days of biotic phase (red line, Fig. 1A). Current density increases over time are typically observed in microbial electrosynthesis systems as the biofilm develops on the cathode[41]. From previous work with similar reactor operation

conditions, it can be predicted that it takes at least 60 days for the current to reach  $-3$  kA/m<sup>3</sup> (without any pre-treatment or potential change)[6,34]. In studies with comparable 3D cathodes and different conditions, it took at least 15 days from starting the system to reaching the current densities measured in this study right after switching to microbial viable conditions (TMM+)[6,15]. By the integration of the TMM HER catalyst, high current density values are reached at day 1 of biotic operation, showing that the start-up time for hydrogen production is shortened. After the TMM- pre-treatment, the current density values were up to  $-90$  kA/m<sup>3</sup> at the start of the biotic phase (Fig. 1A, day 17). These values are close to the highest reported current densities in literature for bio-electrochemical CO<sub>2</sub> reduction systems[20–22] ( $-35$  mA/cm<sup>2</sup> on 2D cathodes, corresponding to  $-117$  kA/m<sup>3</sup> with the cathode thickness used in this study). The high current of the TMM- pre-treated reactors at  $-1.06$  V creates opportunities to operate the reactors at a less negative potential and still create sufficient hydrogen for the growing biofilm[42]. With these improvements, OPEX costs (with less energy investment) may be reduced[43]. In contrast to experiments without HER catalyst, the experiments with HER catalyst show a decrease of current over time during the biotic phase (Fig. 1A, from day 17).

#### 3.2. Metal compound leaching in TMM+ experiments

The slight decrease in hydrogen production over time corresponds with the decrease in the total cathodic current observed in the biotic phase (Fig. 1, 49 % and 40 % decrease in average current for respectively TMM+ and TMM-). Although the hydrogen decrease in the biotic phase could be explained by hydrogen uptake by the microbiome, the current decrease indicates that the HER catalyst performance decreases over time (Fig. 1). Different mechanisms could be causing the apparent catalyst activity decrease: I) leaching, II) biofilm growth and III) poisoning[44]. To investigate leaching, metal concentrations in the catholyte were measured over time during the biotic phase (starting from day 17, Fig. 2). In the TMM- experiments, only Al, Fe and Zn were detected above the detection limit during the biotic phase (Fig. 2B and D). Fe was never above the standard concentration ranges in the biotic catholyte medium which was added over time during the biotic phase with HRT 14 days (310  $\mu$ g/L). Al and Zn are known to deposit on and leach from different reactor parts (e.g. tubing, membrane, Ti wire [34]),

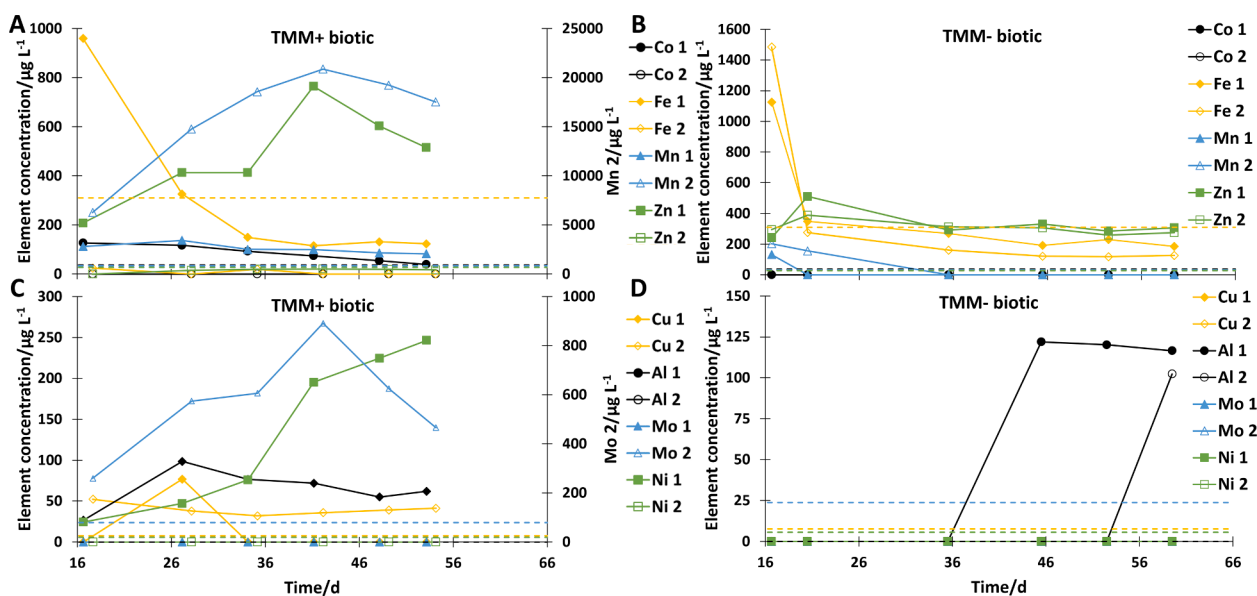


Fig. 2. Average metal concentrations measured with ICP in the catholyte from the start to the end of the biotic phase (day 17-end) of the experiments with cathodes pre-treated with trace metal mix with (TMM+) and without (TMM-) EDTA. The results are presented separately for each replicate experiment (different individual experiments indicated with 1 and 2). The dotted lines indicate the concentrations from the microbial medium.

so the elevated concentrations of Fe, Al and Zn are not indicating leaching of the HER catalyst. These results support that the elements deposited during the metal phase stayed attached to the cathode during the biotic phase of the TMM– experiment.

For the TMM+ experiments, the concentrations of most elements in the catholyte were higher over time compared to TMM– (Fig. 2). Interestingly, the duplicate TMM+ experiments showed significant differences in the concentration trends for Fe, Mn, Mo, Ni and Zn over time. All trace metals, except for Al, Fe and Zn were measured in the catholyte in concentrations higher than in the biotic catholyte medium (Fig. 2A and C). Most elements in the TMM+ experiments did not increase over time, with exception of Mn, Mo, Ni and Zn, indicating those metals leached from the cathode.

The observation that the element concentrations in the TMM+ experiments are higher than in the TMM– experiments (Fig. 2), suggests that the deposition mechanism of the elements to the cathode is affected by the presence of EDTA in the pre-treatment mixture. EDTA slows down electrodeposition by e.g. stabilizing intermediates[45–47], so it is probable that the chelating properties of EDTA also weakened the attachment of different elements to the cathode in the present study.

The other two deactivation mechanisms, biofilm growth and poisoning, are likely to occur during the development of a biofilm on the cathode. The formation of the polymeric layer of the biofilm matrix, secreted by the microorganisms after adhesion on the cathode, can

deactivate the catalyst by blockage of the active site and/or lead to reactant mass transfer limitations[48]. Additionally, the formation of a thick biofilm causes pH gradients[49] which decreases the concentration of protons at the active site of the hydrogen catalyst. Although no significant catalyst deactivation effect of biofilm formation on cathodes has been suggested[50], and several studies even showed improved hydrogen formation after biofilm growth[51–53], the effect of biofilm formation on catalyst stability requires further study. Poisoning can occur from the binding of e.g. N- or S-compounds to the catalyst surface [44,54].  $\text{NH}_4^+$  and  $\text{SO}_4^{2-}$  were added over time during continuous operation to support microbial growth, so poisoning because of chemical binding cannot be excluded either as possible catalyst deactivation mechanism. In conclusion, a combination of leaching, biofilm growth and catalyst poisoning likely decreased the HER catalyst activity over time in the biotic phase.

### 3.3. Successful start-up of microbial activity after pre-treatment

Despite a slight deactivation of the HER catalyst, hydrogen was present in the catholyte bulk throughout the complete biotic phase of the TMM+ and TMM– experiments (Fig. 1B), showing the HER catalyst can work under biotic conditions. In the next step microbial synthesis was performed. To assess the microbial activity with the pre-treated cathodes, the concentrations of volatile fatty acids (VFA) were monitored in

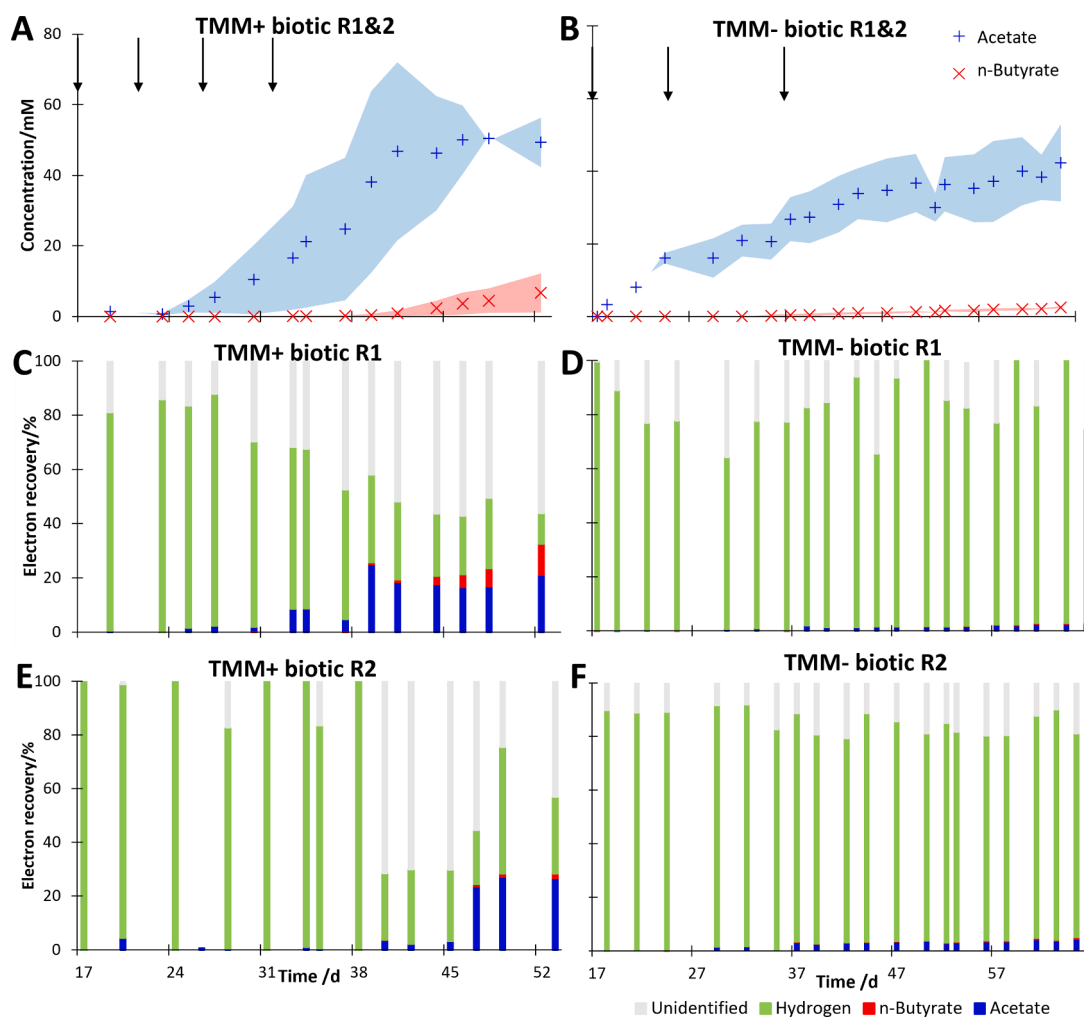


**Fig. 3.** Production of volatile fatty acids and hydrogen over time during the biotic phase in the experiments pre-treated with trace metal mix with (TMM+: A, C and E) and without EDTA (TMM–: B, D and F) shown as catholyte bulk concentrations (A and B) and as a fraction of the measured cathode current (C to F). A and B show averages between duplicate experiments (R1&2) with the difference between duplicates indicated as blue and red areas and inoculation indicated with black arrows, while C to F show the individual reactor data.

the recirculated catholyte over operation time of the biotic phase (starting at day 17, Fig. 3).

In the control reactor, no volatile fatty acids were detected throughout the biotic phase. In the TMM pre-treated reactors, the concentrations of both acetate and n-butyrate increased over time, and production started right after the start of the biotic phase (Fig. 3A and B). From the liquid and gas samples over time and the current, electron recoveries were calculated (see materials and method for calculation). When hydrogen would be the sole consumed as intermediate electron donor, the hydrogen consumption is estimated to be 24 and 27 mmol H<sub>2</sub> per day (3802 and 4197 mol H<sub>2</sub> per m<sup>3</sup> cathode per day), respectively for the TMM+ and TMM- reactors. Besides the detected acetate and n-butyrate, unidentified products are also shown in the electron recovery graphs (Fig. 3C-F). The unidentified electron recoveries (grey bars, Fig. 3C-F) likely account for biomass growth and fractions of the acetate and n-butyrate that could have passed the membrane to the anode compartment. Additionally, methane production below the detection limit of the gas chromatograph (2500 ppm) could have occurred and be part of the unidentified electron recoveries since no chemical inhibitor was added to the catholyte medium. The productivity in both the TMM- and TMM+ pre-treatment experiments shows that the pre-treatments were suitable for successful start-up of bio-electrochemical CO<sub>2</sub>

reduction. However, the cumulative Faradaic efficiency of electrons recovered as acetate and n-butyrate never exceeded 40 % (Fig. 3C-F), so the efficiency of electron transfer into carbon products needs to be improved, for example for lowering to CO<sub>2</sub> supply rate to prevent flush out of hydrogen gas.

#### 3.4. Microbial growth during the biotic phase of the process

The microbial growth both in the liquid phase and on the cathode surface, were monitored via OD<sub>600</sub> measurement and scanning electron microscopy (SEM) analysis, respectively. The optical density values remained quite low (<0.05 OD<sub>600</sub>) throughout the biotic experiment phases (SI Figure S3) compared to other studies without a TMM pre-treatment [21,24]. In the control reactor, the optical density values reached up to 0.06, showing slightly higher concentrations of suspended microorganisms (SI Figure S3). The low concentration of bacteria in the liquid phase of the pre-treated experiments, connected with the microbial activity observed through the volatile fatty acid production (Fig. 3), indicated that after pre-treatment, the microbial growth would mainly be in the aggregated form at the cathode [6], possibly because the most dissolved form of hydrogen would be present near the cathode. The SEM analysis carried out on cathodes samples taken at the end of the biotic

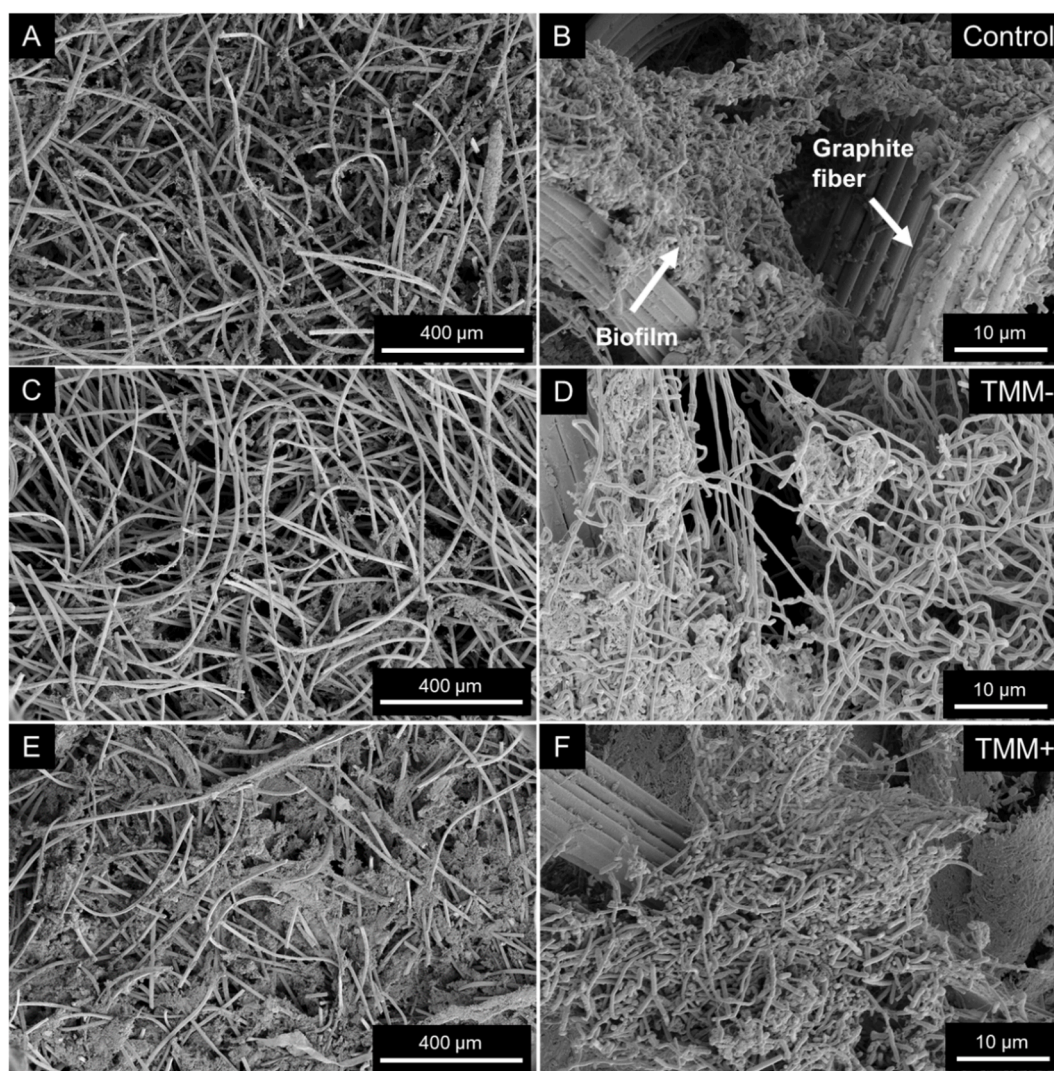


**Fig. 4.** Scanning electron microscopy (SEM) images with two different magnifications of cathode samples taken from the control experiments (A and B), the experiments with cathodes pre-treated with trace metal mix without (TMM-, C and D) and with EDTA (TMM +, E and F). In A, C and E, the biofilm coverage of the cathode is shown. Appearance of a graphite fiber of the carbon felt cathode and the biofilm growing on top are indicated in B. Pictures from duplicate cathodes are shown in SI Figure S4-S6.

phase (day 36 for TMM+ and day 50 for TMM-) showed indeed formation of complex biofilms with different shapes of cells and extracellular polymeric substances (EPS) between different experiments (Fig. 4 with duplicates shown in SI Figure S4-S6).

Within the control experiment, without trace metal mix pre-treatment, biofilm growth on the cathode was observed (Fig. 4A and B), and the coverage of the graphite fibres was similar as the one visualized within the experiment with cathodes pre-treated with TMM- (Fig. 4C and D). However, the biofilm cells' morphology was different. Long filamentous cells growing within the TMM- experiment (Fig. 4D), and less EPS rich clusters in comparison to the control experiment (Fig. 4B and D). In contrast, the biofilm coverage of the cathode surface in the TMM+ pre-treated experiment (Fig. 4E and F) was significantly higher than observed in the control and TMM- experiments, corresponding to the higher productivity observed in the TMM+ experiments (Fig. 3).

### 3.5. Microbial community composition and observation via NGS and FISH

The microbial community composition of the biofilms and liquid samples taken at the end of the process was investigated via next generation sequencing (NGS) of 16S rRNA gene. In all the samples analysed, four main microbial groups were dominant, affiliated to the genera BRH-c20a (phylum *Firmicutes*), *Clostridium sensu stricto* 12, *Methanobacterium* and *Bacteroides* (Table 2).

Members of BRH-c20a (phylum *Firmicutes*) were the dominant group in the biofilms, irrespective of the EDTA addition (Table 2). Even if this genus includes just uncultured representatives (according to Silva database ssu r138.1), its members were previously detected in microbial electrochemical systems[55–58]. In particular, BRH-c20a was identified as a key player in electrochemical CO<sub>2</sub> reduction to acetate, with the electrode as the sole electron donor, while it was not detected when the same inoculum was fed with ethanol as electron donor[57]. BRH-c20a were the dominant bacteria in a study from Gao, Li, Cai, Zhang, Liang, Jiang and Zeng [56] (relative abundance between 48 % and 80 %) associated with slurry-electrode MES producing acetate from hydrogen/carbon dioxide in presence of metal nanoparticles. The high BRH-c20a abundance in presence of metal particles matches with the current study and suggests tolerance for or even use of metal particles as e.g. electron shuttle. Thus, BRH-c20a is likely involved in CO<sub>2</sub> fixation and positively related to acetate production[56], as also highlighted by the

results obtained in our process (Fig. 3).

The genus *Clostridium sensu stricto* 12 was the second dominant group in the biofilm grown in TMM- experiments, while their relative abundance was relatively lower in the TMM+ experiments (Table 2). Members of the genus *Clostridium* are most commonly detected as biocatalysts in BES that can utilize CO<sub>2</sub> as substrate producing acetate[59–61]. Within BES, further elongation of acetate to MCFA is possible thanks to other ssp. of *Clostridium*, such as *Clostridium kluyveri*, which grows on acetate and ethanol via reverse-b-oxidation, producing chain elongated acids like butyrate and caproate[62,63]. *Clostridium* type strains classified under the genus *Clostridium sensu stricto* 12 and reported to catalyse CO<sub>2</sub> fixation and/or produce medium chain fatty acids are *C. kluyveri*[62], *C. ljungdahlii*[64], *C. autoethanogenum*[59], *C. carboxidivorans*[65], *C. tyrobutyricum*[66], *C. pasteurianum*[67] and *C. luti-cellarii*[68].

The *Bacteroides* genus was more abundant in the catholyte than in the cathodic biofilm (Table 2), and members of this genus were previously detected in different microbial electrosynthesis systems. Commonly *Bacteroides* are identified in microbial electrosynthesis as exoelectrogenic bacteria degrading complex substrates to produce acetate and propionate[69–71], and connected with high current generation via extracellular electron transfer and Fe (III) reduction[72,73]. In the human gut, *Bacteroides* were associated with conversion of carbohydrates to fatty acids whilst capturing CO<sub>2</sub>[74].

In both the cathode biofilm and the liquid catholyte the presence/absence of EDTA in the pre-treatment TMM influenced the microbial community composition (Table 2). Focusing on the biofilm, among bacteria, *Erysipelotrichaceae* UCG-004 was identified just without EDTA (Table 2, TMM-), with a relative abundance between 12 and 14 %. While their functional metabolism is still not clear[75], members of the family *Erysipelotrichaceae* were identified in the gut microbiota connected to high concentration of toxic metals[76–78]. The same applies for the genus *Telmatospirillum*, previously detected as active group in hydrogen rich environments[79]. On the contrary, the relative abundance of *Methanobacterium* was lower in both biofilm and liquid samples without EDTA addition (TMM-), indicating that metal chelation is needed for this methanogen to grow and overcome the metal toxicity, which can negatively influence some hydrogenotrophic methanogens [80,81]. Other bacterial groups developed in the biofilm mostly in presence of EDTA (TMM+) were *Pseudomonas*, *Oscillibacter* and *Rikenellaceae* RC9 gut group, all previously detected at biocathodes in different processes[11,82–86]. Although none of the most abundant

**Table 2**

Relative abundances of core operational taxonomic units (OTUs) and their taxonomy classification at the identified level. The 16S rRNA gene analysis by means of Next Generation Sequencing (NGS) was conducted on samples from the cathode biofilm and the liquid catholyte sampled from the two replicate reactors (R1 and R2) for both TMM+ and TMM- experiments at the end of the operation of each reactor. All OTUs < 3 % are summed together and presented as "Other".

Affiliation	TMM+				TMM-			
	R1		R2		R1		R2	
	Biofilm	Liquid catholyte	Biofilm	Liquid catholyte	Biofilm	Liquid catholyte	Biofilm	
<i>Firmicutes</i> BRH-c20a	22.1	8.1	37.3	2.7	33.5	12.2	33.4	
<i>Bacteroides</i>	13.5	30.4	7.8	32.0	7.9	35.9	9.9	
<i>Clostridium sensu stricto</i> 12	13.2	4.8	11.7	10.1	23.6	6.6	23.4	
<i>Methanobacterium</i>	24.2	11.4	22.2	16.7	1.7	1.8	2.2	
<i>Erysipelatoclostridiaceae</i> UCG-004	1.5	0.5	0.7	0.2	12.1	0.4	14.1	
<i>Telmatospirillum</i>	0.2	0.6	0.2	0.5	2.4	13.9	1.1	
<i>Pseudomonas</i>	3.5	11.8	1.2	8.0	0.3	1.7	0.1	
<i>Oscillibacter</i>	1.2	6.3	2.5	10.1	2.1	2.0	2.3	
<i>Methanobrevibacter</i>	3.0	6.3	1.6	3.7	2.4	5.3	2.7	
<i>Azovibrio</i>	0.4	0.3	0.3	0.7	0.4	5.2	1.0	
<i>Sporolactobacillus</i>	0.7	0.5	0.3	1.1	4.6	1.6	2.1	
<i>Rikenellaceae</i> RC9 gut group	4.0	2.0	3.5	0.2	0.1	0.1	0.1	
<i>Sphaerochaeta</i>	2.7	3.8	2.8	2.4	0.3	1.0	1.7	
<i>Achromobacter</i>	0.2	0.7	1.0	3.5	0.0	0.1	0.0	
Other (< 3%)	9.7	12.4	7.2	8.1	8.7	12.2	6.0	

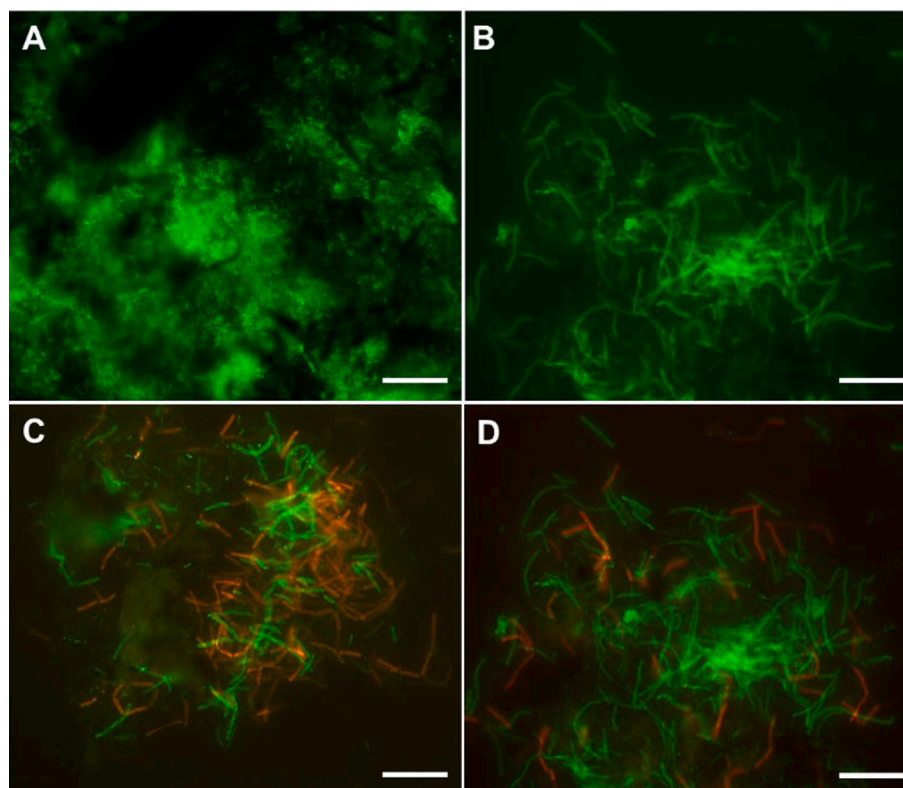


**Fig. 5.** Observation of the bacterial community in biofilms grown on cathodes during the control experiment (A) and with trace metal mix with EDTA (TMM+) pre-treatment (B to D) by Fluorescence in situ hybridization (FISH). The probes applied in are EUB338 (Bacteria, in green) in all the samples showed, and ClostiI (Clostridiales, in red) in A, C and D. The scale bar is 10  $\mu\text{m}$ .

microorganisms are known for hydrogen formation, it cannot be excluded hydrogen was formed biotically, e.g. via biologically excreted hydrogenases[87] or by hydrogenophilic bacteria[88]. Nevertheless, since the overall hydrogen productivity decreased while the volatile fatty acid production increased over time (Fig. 3), it was not expected that biological hydrogen formation had a significant contribution to the hydrogen formation by the trace metal catalysts.

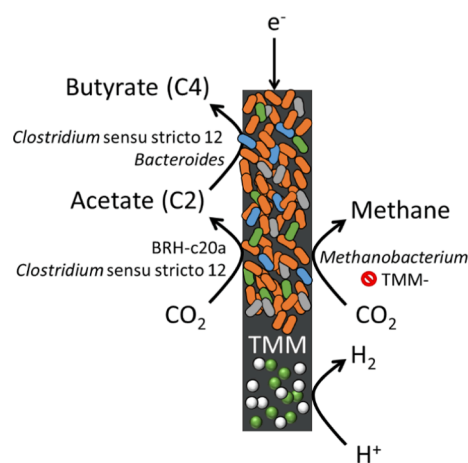
Observing active microbial groups at the end of the TMM+ experiments by applying FISH, based on the morphology it was evident that the addition of trace metals and EDTA stimulated the development of different bacteria in comparison to the control reactors (Fig. 5A and B). By applying probe *ClostiI* (SI Table S3), covering 88 % of the genus *Clostridium sensu stricto* 12 and all the type strains cited above (based on Silva database ssu r138.1), no cells were identified in the control reactor (Fig. 5A), while they constituted a high portion of the whole active bacterial population within TMM+ experiments biofilm (Fig. 5C and D, cells in red). Due to their high relative abundance (Table 2), we can hypothesize the rest of the active biomass visualized in Fig. 5B and C by probe EUB338 belongs to *Firmicutes* BRH-c20a.

Within the biofilm, methanogens affiliated to the order *Methanobacteriales* were identified among the active biomass (SI Figure S7) and a strict association with members of the bacterial community was highlighted in both control and TMM+ reactors (SI Figure S7). Development of methanogens such as *Methanobacterium* and *Methanobrevibacter* was expected, since no 2-bromoethanesulfanoate was added in experiment to optimize the HER catalyst performances, thus it is possible that methane was part of the unidentified products (Fig. 3C-F), as also highlighted by the methanogens activity (SI Figure S7).

### 3.6. EDTA detrimental for hydrogen productivity yet beneficial for microbial synthesis

Based on the differences in current, volatile fatty acid production and

biomass formation between the experiments with pre-treated cathodes (TMM) and the control experiment, it can be concluded that the incorporation of a trace metal mix based HER catalyst is beneficial for a fast start-up and high productivity of volatile fatty acid production from  $\text{CO}_2$ . Interestingly, the pre-treatment with either TMM+ and TMM- showed some differences. The hydrogen production was higher in the TMM- experiments, while the volatile fatty acid productivity was lower and also less biofilm formation was observed in the TMM- experiments compared to the TMM+ experiments. Different explanations could be the reason for the observed differences. For example, the conditions at the cathode surface and in the catholyte are likely different. At the cathode, the hydrogen production will cause local high pH and shear



**Scheme 2.** Representation of the proposed main microbial protagonists' function within the biofilm developed on the cathode in presence of trace metals (TMM).

stress from the bubble formation [16,89], which could have negatively affected the microbial community. Another possibility is a difference in metal toxicity. The ionic form of metals is mostly suggested to be toxic for microorganisms, so the presence of EDTA might lower the toxicity of the trace metals in the catholyte, as also suggested in literature [24,28,90]. It is plausible that metal compounds added during the pre-treatment were more toxic for the microorganisms without the presence of the chelating agent EDTA. An interesting approach to elucidate these hypotheses would be to study metal toxicity or utilization mechanisms in the TMM– experiments.

Overall, a peculiar microbial community with a low number of species (7–8 above 1 % relative abundance, Table 2) developed on top of the cathode when adding trace metals solution. The proposed mechanistic interactions are summarized in Scheme 2. Acetate was the main product of CO<sub>2</sub> utilization, likely via BRH-c20a and *Clostridium* group, while low concentrations of butyrate could come either from chain elongation of acetate by *Clostridium* or from fermentation of organics coming from biomass decay by *Bacteroides* (Scheme 2). Low concentrations of methane were likely formed by *Methanobacterium*, which might be inhibited by the absence of EDTA in the pre-treatment trace metal mix. However, further investigations utilizing additional FISH probes and including the full sequencing of the 16S rRNA gene and the transcriptomic analysis are needed to gain further insights into the metabolism activated with the addition of TMM solution and the generation of a HER catalyst.

#### 4. Conclusions

Here, we demonstrated the feasibility of a hydrogen evolution catalyst formed from microbial trace metals integrated in a bioelectrochemical CO<sub>2</sub> reduction system. The metal mix with (TMM+) and without (TMM–) EDTA showed 10 to 40 times elevated current and hydrogen production compared to a non-pre-treated system during microbial electrosynthesis (TMM–: –90 kA/m<sup>3</sup> and 14 μM hydrogen; TMM+: –20 kA/m<sup>3</sup> and 4 μM hydrogen). The high current at the start of the biotic phase allowed for a fast start-up of microbial activity. Twenty days after start-up of the biotic phase, *n*-butyrate was formed, showing the possibility of CO<sub>2</sub> reduction to C4-compounds in one integrated system. The TMM+ system reached a 36 % electron recovery into C2 and C4 compounds at –20 kA/m<sup>3</sup>. The current density decrease over time was related to metal element leaching. Microbial community analysis showed an active biofilm community on the cathode, which metabolic functions likely correspond to CO<sub>2</sub> conversion into acetate and methane and production of butyrate via either fermentation or chain elongation.

#### CRedit authorship contribution statement

**Sanne M. de Smit:** Writing – original draft, Supervision, Methodology, Funding acquisition, Formal analysis, Conceptualization. **Thomas D. van Mameren:** Writing – review & editing, Investigation, Formal analysis. **Koen van Zwet:** Writing – review & editing, Investigation, Formal analysis. **H. Pieter J. van Veelen:** Writing – review & editing, Formal analysis. **M. Cristina Gagliano:** Writing – review & editing, Writing – original draft, Methodology, Investigation, Formal analysis. **David P.B.T.B. Strik:** Writing – review & editing, Supervision, Funding acquisition, Formal analysis. **Johannes H. Bitter:** Writing – review & editing, Supervision, Funding acquisition, Formal analysis.

#### Declaration of competing interest

The authors declare that they have no known competing financial interests or personal relationships that could have appeared to influence the work reported in this paper.

#### Data availability

Data will be made available online with open access after publication under the doi mentioned in the manuscript

#### Acknowledgements

The authors thank Agnieszka Tomaszewska for practical help to perform FISH analysis at the Microbiology Lab of Wetsus, European Centre of Excellence for Sustainable Water Technology (www.wetsus.nl). Thanks to the Wageningen EM center for facilitation of the SEM images. Financial contribution of WIMEK and Chaincraft BV is greatly acknowledged.

#### Data deposit

The raw data of this study is available in the 4TU database with DOI 10.4121/21591648.

#### Appendix A. Supplementary data

Supplementary data to this article can be found online at <https://doi.org/10.1016/j.bioelechem.2024.108724>.

#### References

- [1] M. Yuan, M.J. Kummer, S.D. Minter, Strategies for bioelectrochemical CO<sub>2</sub> reduction, *Chem. – European J.* 25 (2019) 14258–14266.
- [2] F. Ammam, P.-L. Tremblay, D.M. Lizak, T. Zhang, Effect of tungstate on acetate and ethanol production by the electrosynthetic bacterium *Sporomusa ovata*, *Biotechnol. Biofuels* 9 (2016) 163.
- [3] S. Cheng, D. Xing, D.F. Call, B.E. Logan, Direct biological conversion of electrical current into methane by electromethanogenesis, *Environ. Sci. Tech.* 43 (2009) 3953–3958.
- [4] R. Cai, R.D. Milton, S. Abdellaoui, T. Park, J. Patel, B. Alkotaini, S.D. Minter, Electroenzymatic C-C bond formation from CO<sub>2</sub>, *J. Am. Chem. Soc.* 140 (2018) 5041–5044.
- [5] J.B.A. Arends, S.A. Patil, H. Roume, K. Rabaey, Continuous long-term electricity-driven bioproduction of carboxylates and isopropanol from CO<sub>2</sub> with a mixed microbial community, *J. CO<sub>2</sub> Util.* 20 (2017) 141–149.
- [6] L. Jourdin, S.M.T. Raes, C.J.N. Buisman, D.P.B.T.B. Strik, Critical biofilm growth throughout unmodified carbon felts allows continuous bioelectrochemical chain elongation from CO<sub>2</sub> up to caproate at high current density, *Front. Energy Res.* (2018) 6.
- [7] P. Batlle-Vilanova, R. Ganigué, S. Ramió-Pujol, L. Baneras, G. Jiménez, M. Hidalgo, M.D. Balaguer, J. Colprim, S. Puig, Microbial electrosynthesis of butyrate from carbon dioxide: production and extraction, *Bioelectrochemistry* 117 (2017) 57–64.
- [8] S. Bajracharya, A. ter Heijne, X. Dominguez Benetton, K. Vanbroekhoven, C. J. Buisman, D.P. Strik, D. Pant, Carbon dioxide reduction by mixed and pure cultures in microbial electrosynthesis using an assembly of graphite felt and stainless steel as a cathode, *Bioresour. Technol.* 195 (2015) 14–24.
- [9] T. Zhang, H. Nie, T.S. Bain, H. Lu, M. Cui, O.L. Snoeyenbos-West, A.E. Franks, K. P. Nevin, T.P. Russell, D.R. Lovley, Improved cathode materials for microbial electrosynthesis, *Energ. Environ. Sci.* 6 (2013) 217–224.
- [10] B. Witholt, B. Kessler, Perspectives of medium chain length poly (hydroxyalkanoates), a versatile set of bacterial bioplastics, *Curr. Opin. Biotechnol.* 10 (1999) 279–285.
- [11] S. Bajracharya, S. Srikanth, G. Mohanakrishna, R. Zacharia, D.P. Strik, D. Pant, Biotransformation of carbon dioxide in bioelectrochemical systems: state of the art and future prospects, *J. Power Sources* 356 (2017) 256–273.
- [12] D.R. Lovley, Live wires: direct extracellular electron exchange for bioenergy and the bioremediation of energy-related contamination, *Energ. Environ. Sci.* 4 (2011) 4896–4906.
- [13] P. Levy, J. Sanderson, R. Kispert, D. Wise, Biorefining of biomass to liquid fuels and organic chemicals, *Enzyme Microb. Technol.* 3 (1981) 207–215.
- [14] C.M. Spirito, H. Richter, K. Rabaey, A.J. Stams, L.T. Angenent, Chain elongation in anaerobic reactor microbiomes to recover resources from waste, *Curr. Opin. Biotechnol.* 27 (2014) 115–122.
- [15] L. Jourdin, T. Grieger, J. Monetti, V. Flexer, S. Freguia, Y. Lu, J. Chen, M. Romano, G.G. Wallace, J. Keller, High acetic acid production rate obtained by microbial electrosynthesis from carbon dioxide, *Environ. Sci. Technol.* 49 (2015) 13566–13574.
- [16] E. Blanchet, F. Duquenne, Y. Rafrafi, L. Etcheverry, B. Erable, A. Bergel, Importance of the hydrogen route in up-scaling electrosynthesis for microbial CO<sub>2</sub> reduction, *Energ. Environ. Sci.* 8 (2015) 3731–3744.
- [17] S.T. Boto, B. Bardl, F. Harnisch, M.A. Rosenbaum, Microbial electrosynthesis with *Clostridium ljungdahlii* benefits from hydrogen electron mediation and permits a greater variety of products, *Green Chem.* (2023).

- [18] Z. Zhou, Z. Pei, L. Wei, S. Zhao, X. Jian, Y. Chen, Electrocatalytic hydrogen evolution under neutral pH conditions: current understandings, recent advances, and future prospects, *Energy. Environ. Sci.* 13 (2020) 3185–3206.
- [19] V. Flexer, L. Jourdin, Purposely designed hierarchical porous electrodes for high rate microbial electrosynthesis of acetate from carbon dioxide, *Acc. Chem. Res.* 53 (2020) 311–321.
- [20] C. Liu, B.C. Colón, M. Ziesack, P.A. Silver, D.G. Nocera, Water splitting–biosynthetic system with CO<sub>2</sub> reduction efficiencies exceeding photosynthesis, *Science* 352 (2016) 1210–1213.
- [21] F. Kracke, A.B. Wong, K. Maegaard, J.S. Deutzmann, M.A. Hubert, C. Hahn, T. F. Jaramillo, A.M. Spormann, Robust and biocompatible catalysts for efficient hydrogen-driven microbial electrosynthesis, *Commun. Chem.* 2 (2019) 45.
- [22] G. Wang, Q. Huang, T.-S. Song, J. Xie, Enhancing microbial electrosynthesis of acetate and butyrate from CO<sub>2</sub> reduction involving engineered *Clostridium ljungdahlii* with a nickel-phosphide-modified electrode, *Energy Fuel* 34 (2020) 8666–8675.
- [23] S. Tian, H. Wang, Z. Dong, Y. Yang, H. Yuan, Q. Huang, T.-S. Song, J. Xie, Mo 2 C-induced hydrogen production enhances microbial electrosynthesis of acetate from CO<sub>2</sub> reduction, *Biotechnol. Biofuels* 12 (2019) 1–12.
- [24] K.-R. Chatzipanagiotou, L. Jourdin, J.H. Bitter, D.P. Strik, Concentration-dependent effects of nickel doping on activated carbon biocathodes, *Cataly. Sci. Technol.* 12 (2022) 2500–2518.
- [25] Z. Chen, A.G. Rodriguez, P. Nunez, D. van Houtven, D. Pant, J. Vaes, Experimental investigation of anion exchange membrane water electrolysis for a tubular microbial electrosynthesis cell design, *Catal. Commun.* 170 (2022) 106502.
- [26] S.M. de Smit, T.D. van Mameren, Y. Xie, D.P.B.T.B. Strik, J.H. Bitter, Trace metals from microbial growth media form in situ electro-catalysts, *Electrochim. Acta* 462 (2023) 142722.
- [27] S. Zhang, J. Jiang, H. Wang, F. Li, T. Hua, W. Wang, A review of microbial electrosynthesis applied to carbon dioxide capture and conversion: The basic principles, electrode materials, and bioproducts, *J. CO<sub>2</sub> Util.* 51 (2021) 101640.
- [28] G.M. Gadd, A.J. Griffiths, Microorganisms and heavy metal toxicity, *Microb. Ecol.* 4 (1977) 303–317.
- [29] J. Wingender, T.R. Neu, H.-C. Flemming, in: What are bacterial extracellular polymeric substances?, *Microbial extracellular polymeric substances*, Springer, 1999, pp. 1–19.
- [30] S.W. Ragsdale, E. Pierce, Acetogenesis and the Wood-Ljungdahl pathway of CO<sub>2</sub> fixation, *Biochim. Biophys. Acta (BBA)-Proteins Proteomics* 1784 (2008) 1873–1898.
- [31] F. Kracke, I. Vassilev, J.O. Krömer, Microbial electron transport and energy conservation—the foundation for optimizing bioelectrochemical systems, *Front. Microbiol.* 6 (2015) 575.
- [32] H. Irving, R. Williams, Order of stability of metal complexes, *Nature* 162 (1948) 746–747.
- [33] K.J. Waldron, J.C. Rutherford, D. Ford, N.J. Robinson, Metalloproteins and metal sensing, *Nature* 460 (2009) 823–830.
- [34] S.M. de Smit, C.J. Buisman, J.H. Bitter, D.P. Strik, Cyclic Voltammetry is invasive on microbial electrosynthesis, *ChemElectroChem* 8 (2021) 3384–3396.
- [35] J. Oudar, Sulfur adsorption and poisoning of metallic catalysts, *Cataly. Rev.—Sci. Eng.* 22 (1980) 171–195.
- [36] R. Sander, Compilation of Henry's law constants (version 4.0) for water as solvent, *Atmos. Chem. Phys.* 15 (2015) 4399–4981.
- [37] E. Bolyen, J.R. Rideout, M.R. Dillon, N.A. Bokulich, C.C. Abnet, G.A. Al-Ghalith, H. Alexander, E.J. Alm, M. Arumugam, F. Asnicar, Reproducible, interactive, scalable and extensible microbiome data science using QIIME 2, *Nat. Biotechnol.* 37 (2019) 852–857.
- [38] P. Hugenholz, G.W. Tyson, L.L. Blackall, in: Design and evaluation of 16S rRNA-targeted oligonucleotide probes for fluorescence in situ hybridization, *Gene probes*, Springer, 2002, pp. 29–42.
- [39] D. Greuter, A. Loy, M. Horn, T. Rattei, probeBase—an online resource for rRNA-targeted oligonucleotide probes and primers: new features 2016, *Nucleic Acids Res.* 44 (2016) D586–D589.
- [40] D.A. Wiesenburg, N.L. Guinasso Jr, Equilibrium solubilities of methane, carbon monoxide, and hydrogen in water and sea water, *J. Chem. Eng. Data* 24 (1979) 356–360.
- [41] P. Izadi, J.-M. Fontmorin, A. Godain, E.H. Yu, I.M. Head, Parameters influencing the development of highly conductive and efficient biofilm during microbial electrosynthesis: the importance of applied potential and inorganic carbon source, *NPJ Biofilms Microbiomes*. 6 (2020) 1–15.
- [42] H.V. Hamelers, A. Ter Heijne, T.H. Sleutels, A.W. Jeremiasse, D.P. Strik, C. J. Buisman, New applications and performance of bioelectrochemical systems, *Appl. Microbiol. Biotechnol.* 85 (2010) 1673–1685.
- [43] L. Jourdin, J. Sousa, N.V. Stralen, D.P.B.T.B. Strik, Techno-economic assessment of microbial electrosynthesis from CO<sub>2</sub> and/or organics: An interdisciplinary roadmap towards future research and application, *Appl. Energy* 279 (2020).
- [44] J.P. Lange, Renewable feedstocks: the problem of catalyst deactivation and its mitigation, *Angew. Chem. Int. Ed.* 54 (2015) 13186–13197.
- [45] L. Dong, P. Wang, H. Yu, EDTA-assisted synthesis of amorphous BiSx nanodots for improving photocatalytic hydrogen-evolution rate of TiO<sub>2</sub>, *J. Alloy. Compd.* 887 (2021) 161425.
- [46] Y. Deng, C. Ye, G. Chen, B. Tao, H. Luo, N. Li, EDTA-assisted hydrothermal synthesis of flower-like CoSe<sub>2</sub> nanorods as an efficient electrocatalyst for the hydrogen evolution reaction, *J. Energy Chem.* 28 (2019) 95–100.
- [47] X. Yu, J. Yang, X. Ren, Z. Sui, Influences of pH and EDTA additive on the structure of Ni films electrodeposited by using bubble templates as electrocatalysts for hydrogen evolution reaction, *Membranes* 11 (2021) 165.
- [48] C. Hammond, Intensification studies of heterogeneous catalysts: probing and overcoming catalyst deactivation during liquid phase operation, *Green Chem.* 19 (2017) 2711–2728.
- [49] A. De Lichtervelde, A. Ter Heijne, H. Hamelers, P. Biesheuvel, J. Dykstra, Theory of ion and electron transport coupled with biochemical conversions in an electroactive biofilm, *Phys. Rev. Appl.* 12 (2019) 014018.
- [50] H. Yuan, Y. Hou, I.M. Abu-Reesh, J. Chen, Z. He, Oxygen reduction reaction catalysts used in microbial fuel cells for energy-efficient wastewater treatment: a review, *Mater. Horiz.* 3 (2016) 382–401.
- [51] L. Jourdin, Y. Lu, V. Flexer, J. Keller, S. Freguia, Biologically induced hydrogen production drives high rate/high efficiency microbial electrosynthesis of acetate from carbon dioxide, *ChemElectroChem* 3 (2016) 581–591.
- [52] E. Perona-Vico, L. Feliu-Paradedá, S. Puig, L. Bañeras, Bacteria coated cathodes as an in-situ hydrogen evolving platform for microbial electrosynthesis, *Sci. Rep.* 10 (2020) 1–11.
- [53] C.W. Marshall, D.E. Ross, E.B. Fichot, R.S. Norman, H.D. May, Long-term operation of microbial electrosynthesis systems improves acetate production by autotrophic microbiomes, *Environ. Sci. Tech.* 47 (2013) 6023–6029.
- [54] M.V. Twigg, M.S. Spencer, Deactivation of supported copper metal catalysts for hydrogenation reactions, *Appl. Catal. A* 212 (2001) 161–174.
- [55] M. Ispato, P. Dessì, C. Sánchez, S. Mills, U.Z. Ijaz, F. Asunis, D. Spiga, G. De Gioannis, M. Mascia, G. Collins, Propionate production by bioelectrochemically-assisted lactate fermentation and simultaneous CO<sub>2</sub> recycling, *Front. Microbiol.* 11 (2020) 599438.
- [56] Y. Gao, Z. Li, J. Cai, L. Zhang, Q. Liang, Y. Jiang, R.J. Zeng, Metal nanoparticles increased the lag period and shaped the microbial community in slurry-electrode microbial electrosynthesis, *Sci. Total Environ.* 156008 (2022).
- [57] Y. Jiang, N. Chu, D.-K. Qian, R.J. Zeng, Microbial electrochemical stimulation of caproate production from ethanol and carbon dioxide, *Bioresour. Technol.* 295 (2020) 122266.
- [58] N. Chu, Q. Liang, W. Zhang, Z. Ge, W. Hao, Y. Jiang, R.J. Zeng, Waste C<sub>1</sub> gases as alternatives to pure CO<sub>2</sub> improved the microbial electrosynthesis of C<sub>4</sub> and C<sub>6</sub> carboxylates, *ACS Sustain. Chem. Eng.* 8 (2020) 8773–8782.
- [59] J.K. Heffernan, K. Valgepea, R. de Souza Pinto, I. Lemgruber, M. Casini, R. Plan, S. D. Tappel, M. Simpson, L.K. Köpke, E.M. Nielsen, Enhancing CO<sub>2</sub>-valorization using *Clostridium autoethanogenum* for sustainable fuel and chemicals production, *Front. Bioeng. Biotechnol.* 8 (2020) 204.
- [60] B.Y. Jeon, I.L. Jung, D.H. Park, Conversion of carbon dioxide to metabolites by *Clostridium acetobutylicum* KCTC1037 cultivated with electrochemical reducing power, *Adv. Microbiol.* 2 (2012) 332.
- [61] C. Im, K. Valgepea, O. Modin, Y. Nygård, *Clostridium ljungdahlii* as a biocatalyst in microbial electrosynthesis—Effect of culture conditions on product formation, *Bioresour. Technology Reports* 19 (2022) 101156.
- [62] M.V. Reddy, S.V. Mohan, Y.-C. Chang, Medium-chain fatty acids (MCFA) production through anaerobic fermentation using *Clostridium kluyveri*: effect of ethanol and acetate, *Appl. Biochem. Biotechnol.* (2017) 1–12.
- [63] L.A. Kucek, C.M. Spirito, L.T. Angenent, High n-caprylate productivities and specificities from dilute ethanol and acetate: chain elongation with microbiomes to upgrade products from syngas fermentation, *Energy. Environ. Sci.* 9 (2016) 3482–3494.
- [64] M. Köpke, C. Held, S. Hujer, H. Liesegang, A. Wiezer, A. Wollherr, A. Ehrenreich, W. Liebl, G. Gottschalk, P. Dürre, *Clostridium ljungdahlii* represents a microbial production platform based on syngas, *Proc. Natl. Acad. Sci.* 107 (2010) 13087–13092.
- [65] Y. Shen, R. Brown, Z. Wen, Syngas fermentation of *Clostridium carboxidivoran* P7 in a hollow fiber membrane biofilm reactor: Evaluating the mass transfer coefficient and ethanol production performance, *Biochem. Eng. J.* 85 (2014) 21–29.
- [66] Y. Zhu, S.T. Yang, Adaptation of *Clostridium tyrobutyricum* for enhanced tolerance to butyric acid in a fibrous-bed bioreactor, *Biotechnol. Prog.* 19 (2003) 365–372.
- [67] M. Atasoy, Z. Cetecioglu, Butyric acid dominant volatile fatty acids production: bio-augmentation of mixed culture fermentation by *Clostridium butyricum*, *J. Environ. Chem. Eng.* 8 (2020) 104496.
- [68] Q. Wang, C.D. Wang, C.H. Li, J.G. Li, Q. Chen, Y.Z. Li, *Clostridium luticellarii* sp. nov., isolated from a mud cellar used for producing strong aromatic liquors, *Int. J. Syst. Evol. Microbiol.* 65 (2015) 4730–4733.
- [69] S. Adamberg, K. Tomson, H. Vija, M. Puurand, N. Kabanova, T. Visnapuu, E. Jögi, T. Alamäe, K. Adamberg, Degradation of fructans and production of propionic acid by Bacteroides thetaiotaomicron are enhanced by the shortage of amino acids, *Front. Nutr.* 1 (2014) 21.
- [70] J.A. Albaracin-Arias, C.-P. Yu, T. Maeda, W.V. Quintero, V. Sanchez-Torres, Microbial community dynamics and electricity generation in MFCs inoculated with POME sludges and pure electrogenic culture, *Int. J. Hydrogen Energy* 46 (2021) 36903–36916.
- [71] T.-J. Park, W. Ding, S. Cheng, M.S. Brar, A.P.Y. Ma, H.M. Tun, F.C. Leung, Microbial community in microbial fuel cell (MFC) medium and effluent enriched with purple photosynthetic bacterium (*Rhodospseudomonas* sp), *AMB Express* 4 (2014) 1–8.
- [72] P.T. Ha, T.K. Lee, B.E. Rittmann, J. Park, I.S. Chang, Treatment of alcohol distillery wastewater using a Bacteroidetes-dominant thermophilic microbial fuel cell, *Environ. Sci. Tech.* 46 (2012) 3022–3030.
- [73] Y. Xiao, Y. Zheng, S. Wu, E.-H. Zhang, Z. Chen, P. Liang, X. Huang, Z.-H. Yang, I.-S. Ng, B.-Y. Chen, Pyrosequencing reveals a core community of anodic bacterial biofilms in bioelectrochemical systems from China, *Front. Microbiol.* 6 (2015) 1410.

- [74] M.A. Fischbach, J.L. Sonnenburg, Eating for two: how metabolism establishes interspecies interactions in the gut, *Cell Host Microbe* 10 (2011) 336–347.
- [75] J. Wu, M. Liu, M. Zhou, L. Wu, H. Yang, L. Huang, C. Chen, Isolation and genomic characterization of five novel strains of Erysipelotrichaceae from commercial pigs, *BMC Microbiol.* 21 (2021) 1–12.
- [76] M. Shao, Y. Zhu, Long-term metal exposure changes gut microbiota of residents surrounding a mining and smelting area, *Sci. Rep.* 10 (2020) 1–9.
- [77] J. Breton, S. Massart, P. Vandamme, E. De Brandt, B. Pot, B. Foligné, Ecotoxicology inside the gut: impact of heavy metals on the mouse microbiome, *BMC Pharmacol. Toxicol.* 14 (2013) 1–11.
- [78] J.B. Richardson, B.C. Dancy, C.L. Horton, Y.S. Lee, M.S. Madejczyk, Z.Z. Xu, G. Ackermann, G. Humphrey, G. Palacios, R. Knight, Exposure to toxic metals triggers unique responses from the rat gut microbiota, *Sci. Rep.* 8 (2018) 1–12.
- [79] S. Esquivel-Elizondo, A.G. Delgado, R. Krajmalnik-Brown, Evolution of microbial communities growing with carbon monoxide, hydrogen, and carbon dioxide, *FEMS Microbiol. Ecol.* 93 (2017).
- [80] K.F. Jarrell, M. Saulnier, A. Ley, Inhibition of methanogenesis in pure cultures by ammonia, fatty acids, and heavy metals, and protection against heavy metal toxicity by sewage sludge, *Can. J. Microbiol.* 33 (1987) 551–554.
- [81] J. Sanchez, L. Valle, F. Rodriguez, M. Morinigo, J. Borrego, Inhibition of methanogenesis by several heavy metals using pure cultures, *Lett. Appl. Microbiol.* 23 (1996) 439–444.
- [82] K. Rabaey, N. Boon, S.D. Siciliano, M. Verhaege, W. Verstraete, Biofuel cells select for microbial consortia that self-mediate electron transfer, *Appl. Environ. Microbiol.* 70 (2004) 5373–5382.
- [83] V. Kugarajah, J. Solomon, K. Rajendran, S. Dharmalingam, Enhancement of nitrate removal and electricity generation in microbial fuel cell using eggshell supported biocathode, *Process Biochem.* 113 (2022) 1–10.
- [84] C. Santoro, S. Babanova, P. Cristiani, K. Artyushkova, P. Atanassov, A. Bergel, O. Bretschger, R.K. Brown, K. Carpenter, A. Colombo, How comparable are microbial electrochemical systems around the globe? An Electrochemical and microbiological cross-laboratory study, *ChemSusChem* 14 (2021) 2313–2330.
- [85] C.H. Im, C. Kim, Y.E. Song, S.E. Oh, B.H. Jeon, J.R. Kim, Electrochemically enhanced microbial CO conversion to volatile fatty acids using neutral red as an electron mediator, *Chemosphere* 191 (2018) 166–173.
- [86] S. Seveda, S. Sharma, C. Joshi, L. Pandey, N. Tyagi, I. Abu-Reesh, T. Sreerishnan, Biofilm formation and electron transfer in bioelectrochemical systems, *Environ. Technol. Rev.* 7 (2018) 220–234.
- [87] J.S. Deutzmann, M. Sahin, A.M. Spormann, Extracellular enzymes facilitate electron uptake in biocorrosion and bioelectrosynthesis, *mBio*, 6 (2015).
- [88] M. Villano, L. De Bonis, S. Rossetti, F. Aulenta, M. Majone, Bioelectrochemical hydrogen production with hydrogenophilic dechlorinating bacteria as electrocatalytic agents, *Bioresour. Technol.* 102 (2011) 3193–3199.
- [89] E.V. LaBelle, H.D. May, Energy Efficiency and Productivity Enhancement of Microbial Electrosynthesis of Acetate, *Front. Microbiol.* 8 (2017) 756.
- [90] K.R. Chatzipanagiotou, L. Jourdin, C.J.N. Buisman, D.P.B.T.B. Strik, J.H. Bitter, CO<sub>2</sub> Conversion by Combining a Copper Electrocatalyst and Wild-type Microorganisms, *ChemCatChem* 12 (2020) 3900–3912.



**Koen van Zwet** is a recent graduate of two master's programmes at Wageningen university. In his education, he combined the biotechnology programme, focused on process engineering, with a bioinformatics programme focused on synthetic biology and cell modelling. During his studies, he developed an interest in process design, sustainability and python, with the goal of finding an innovative solution for the challenges he encountered. Currently, Koen is employed as a consultant in the pharmaceutical industry, tackling various projects in the design and validation of production processes.



**H. Pieter J. van Veelen** obtained his MSc degree in Biology at Wageningen University and Research and obtained his PhD at University of Groningen with his research on avian host-microbiome ecology. Currently, he is Head of the Laboratory for Microbiology and Scientific Project Manager at Wetsus in the Netherlands. His research integrates bioinformatics, molecular biology and microbial ecology in the fields of water and environmental technology.



**M. Cristina Gagliano** is Theme Coordinator for Biofilms research at Wetsus, Netherlands. During her PhD in Environmental Sciences (National Research Council, Italy) and her Postdoctoral research (Wageningen University and Research, Netherlands) she worked on anaerobic digestion and the related microbial community, with focus on extracellular polymeric substance (EPS), developing microscopy methods for their identification. Her research currently focuses on different fields of water technology, from biological treatment of wastewater to production/distribution of drinking water. She is supervisor of six PhD students and two postdocs, with several collaborations (University of Groningen, Wageningen University and Research, University of Twente, University of Galway).



**David P.B.T.B. Strik** obtained his PhD in Anaerobic Digestion from BOKU University in Austria in 2004 and completed his MSc in Environmental Sciences at Wageningen University in 1999. Currently, his team is devoted to unlocking the potential of microorganisms within engineered open-culture bioreactors. Their objective is to convert organic, bioplastic, or CO<sub>2</sub> waste streams into valuable products, such as volatile fatty acids, through innovative bio(electro)chemical technologies. As an environmental technologist, his passion lies in exploring and contributing to the generation of knowledge, education, and the advancement of biorefinery approaches that promote the circular economy.



**Johannes H. Bitter** holds an MSc (1993) in organic chemistry and PhD (1997) in heterogeneous catalysis. After his PhD Harry joined the Utrecht University as assistant professor where he continued working in the field of heterogeneous catalysis first focusing on the use of X-Ray spectroscopy and later focusing on the use of carbon-based catalysts both in fossil feedstock conversion and in biomass-based conversion. Since 2013 Harry is full professor at Wageningen University and Research in the Netherlands where he holds the chair Biobased Chemistry and Technology and focuses on catalytic biomass-based conversion (and extraction) processes on multiple length scales.



**Sanne M. de Smit** works as a Postdoc researcher at the Wageningen University. She got a Msc degree (2018) in Biotechnology with a thesis on microbial chain elongation and earned her PhD degree (2023) on the topic of Microbial Electrosynthesis from a self-obtained WIMEK grant. Her main research interests are bio-electrochemical solutions for treatment or reutilisation of various waste streams, e.g. CO<sub>2</sub>, H<sub>2</sub>S, NH<sub>4</sub><sup>+</sup>. Within the field of bio-electrochemistry, she focusses on the combination of chemical and microbial catalysis within bio-electrochemical systems and the characterization of local conditions and gradients by e.g. microsensor measurements.



**Thomas D. van Mameren** holds a bachelor's in chemistry and a Master's in Biobased Sciences from Wageningen. During his thesis he focussed on microbial electrosynthesis. Where the impact of trace metals & EDTA on the hydrogen evolution reaction and fatty acid production was investigated. Currently working as a researcher at ChainCraft, focussing on the upscaling of the Chain Elongation process.